

RESEARCH ARTICLE

Differences in titin segmental elongation between passive and active stretch in skeletal muscle

Michael M. DuVall^{1,2}, Azim Jinha¹, Gudrun Schappacher-Tilp³, Timothy R. Leonard¹ and Walter Herzog¹

ABSTRACT

Since the 1950s, muscle contraction has been explained using a two-filament system in which actin and myosin exclusively dictate active force in muscle sarcomeres. Decades later, a third filament called titin was discovered. This titin filament has recently been identified as an important regulator of active force, but has yet to be incorporated into contemporary theories of muscle contraction. When sarcomeres are actively stretched, a substantial and rapid increase in force occurs, which has been suggested to arise in part from titin–actin binding that is absent in passively stretched sarcomeres. However, there is currently no direct evidence for such binding within muscle sarcomeres. Therefore, we aimed to determine whether titin binds to actin in actively but not in passively stretched sarcomeres by observing length changes of proximal and distal titin segments in the presence and absence of calcium. We labeled I-band titin with fluorescent F146 antibody in rabbit psoas myofibrils and tracked segmental elongations during passive (no calcium) and active (high calcium) stretch. Without calcium, proximal and distal segments of titin elongated as expected based on their free spring properties. In contrast, active stretch differed statistically from passive stretch, demonstrating that calcium activation increases titin segment stiffness, but not in an actin-dependent manner. The consistent elongation of the proximal segment was contrary to what was expected if titin's proximal segment was attached to actin. This rapid calcium-dependent change in titin stiffness likely contributes to active muscle force regulation in addition to actin and myosin.

KEY WORDS: Sarcomere, Calcium, Force enhancement, Muscle contraction

INTRODUCTION

Muscle contraction and force production are largely explained by the sliding filament (Huxley and Hanson, 1954; Huxley and Niedergerke, 1954) and cross-bridge theories (Huxley, 1957, 1969; Huxley and Simmons, 1971), which detail the intricacies of actin versus myosin filament sliding and cross-bridge kinetics during muscle activation. However, experimental evidence that cannot be explained within the framework of these theories has existed equally as long (Abbott and Aubert, 1952). This is particularly evident for eccentric contractions, in which muscles are actively lengthened.

Eccentrically contracting muscles are capable of producing steady-state forces as much as twice the force that they can produce isometrically at the corresponding length and activation (Edman et al., 1982; Leonard and Herzog, 2010). In fact, these experimentally high forces are not theoretically possible at any length based on the cross-bridge theory (Walcott and Herzog, 2008). This increased steady-state force following active stretching beyond that observed isometrically at the corresponding length and activation has been termed residual force enhancement, and has been seen in preparations including whole muscles (Herzog and Leonard, 2000, 2002), single fibers (Edman et al., 1978, 1982; Sugi and Tsuchiya, 1988), myofibrils (Joumaa et al., 2008b; Leonard and Herzog, 2010) and single sarcomeres (Leonard et al., 2010; Rassier and Pavlov, 2011). Residual force enhancement depends on stretch magnitude (Abbott and Aubert, 1952; Herzog and Leonard, 2002) and muscle length (Edman et al., 1982; Joumaa et al., 2008b), but is largely independent of stretch speed (Edman et al., 1978; Sugi and Tsuchiya, 1988). As mechanically isolated sarcomeres are capable of residual force enhancement, it can be reasoned that the mechanism responsible must be contained within the sarcomere.

About 25 years after the formulation of the sliding filament and cross-bridge theories, a third filamentous protein called connectin (Maruyama, 1976; Maruyama et al., 1977) or titin (Maruyama et al., 1981; Wang et al., 1979) was discovered. In the I-band region of sarcomeres, titin is a molecular spring with serially arranged elements of different stiffness. These elements dictate titin's response to stretch, such that the proximal and distal immunoglobulin (Ig) regions first straighten under low force, while the PEVK region becomes the primary force-producing element thereafter (Trombitás et al., 1998).

Recently, it has been proposed that titin might also contribute to active force in addition to actin–myosin-based forces through titin binding to actin, thereby reducing titin's spring length and increasing its stiffness (Leonard and Herzog, 2010; Linke et al., 1997; Nishikawa et al., 2012). There is, however, no direct experimental support for titin–actin binding, although *in vitro* work suggests that titin–actin binding might be a distinct possibility (Kellermayer and Granzier, 1996).

The purpose of our study was to observe segmental changes in titin's I-band within the sarcomeres of passively and actively stretched myofibrils to evaluate titin–actin binding. Using immunofluorescence, we demarcated titin into proximal and distal segments with site-specific F146 titin antibodies and tracked these segments during passive and active stretch. We hypothesized that I-band titin would elongate as expected from known stress–strain properties during passive stretch. However, this behavior would be different during active stretch, if titin's proximal segment length change was limited via actin binding. Our findings indicate that the I-band proximal segment length increased rapidly with calcium-activated stretch, altering titin's mechanical properties and force

¹Human Performance Lab., University of Calgary, Calgary, AB, Canada T2N 1N4.

²Center for Bioengineering Innovation, Northern Arizona University, Flagstaff, AZ 86011, USA. ³Department of Mathematics and Scientific Computing,

Karl-Franzens-Universität Graz, 8010 Graz, Austria.

*Author for correspondence (mmduvall@ucalgary.ca)

© M.M.D., 0000-0001-9938-7468

contribution in a calcium-, cross-bridge- and sarcomere length-dependent manner. However, our observations do not support an interaction of proximal or distal segments with actin.

MATERIALS AND METHODS

Myofibril preparations

Ethical approval for all experiments was granted by the Life and Environmental Sciences Animal Care Committee at the University of Calgary. Six month old female New Zealand white rabbits were euthanized, and the psoas muscle was freshly harvested and cut into small strips, fixed in place with sutures to maintain *in vivo* sarcomere lengths (SLs) and chemically skinned overnight using solutions detailed elsewhere (Joumaa et al., 2007). Notable solution changes from Joumaa et al. (2007) included reduced concentrations of EGTA (2 and 1 mmol l⁻¹) and calcium (0 and 3.5 mmol l⁻¹) in relaxing and activating solutions, respectively, purchased from Sigma Aldrich® (St Louis, MO, USA). Myofibrils were prepared fresh on the day of experiments by homogenizing muscle samples in rigor using a mechanical blender (Model PRO250, Pro Scientific, Oxford, CT, USA). Primary F146.9B9 (hereafter F146; 1:35, ALX-BC-3010-S, Farmingdale, Enzo Life Sciences, NY, USA) and anti-myomesin (1:65, mMaC myomesin B4, Developmental Studies Hybridoma Bank, Iowa City, IA, USA) antibodies, specific for the PEVK region of titin and M-line myomesin, respectively, were added for 20 min at 4°C. The titin F146 epitope was located approximately in the distal one-third of the PEVK region. Following antibody labeling, a secondary Alexa Fluor® 488 dye (A32723, Invitrogen, Carlsbad, CA, USA) was introduced for another 20 min at 4°C.

Protocol

Myofibril stretch was performed using a piezo motor (Physik Instrumente GmbH & Co, Karlsruhe, Germany) controlled using custom-written LabView® software (National Instruments Corp., Austin, TX, USA). A stretch of 0.1 µm per sarcomere per second, or about 5% of the sarcomere resting length per second, was used. The myofibrils were activated by a directed stream of activation solution (Colomo et al., 1997), and remained activated for the duration of stretch. All experiments were performed at room temperature. Experiments were recorded using a Retiga™ 4000DC video camera (QImaging, Surrey, BC, Canada) at 200× (NA 1.3, Olympus, Japan) with a pixel resolution of 37 nm.

Analysis

The fluorescent antibody (Ab) bands were tracked relative to the M-line and Z-line for the same consecutive sarcomeres of the myofibril throughout the entire stretch using ImageJ (1.47V, NIH, Bethesda, MA, USA). Sarcomeres were defined from one M-line myomesin antibody to the next consecutive M-line marker. Titin F146 primary antibody in the PEVK-distal Ig region separated I-band titin into proximal (Z-line to proximal PEVK) and distal (distal PEVK to the A-band edge) segments. Lengths of distal segments were calculated relative to the A-band edge, as the distance from the titin antibody to the labeled M-line, minus 0.8 µm (half thick filament length). Lengths of proximal and distal segments were averaged for the two measurements collected for each sarcomere.

Here, we refer to a distinct change in slope of proximal or distal segments with stretch as a ‘transition point’. These transition points occur when segment contour lengths are achieved, resulting in a change in titin segment extensibility (Wang et al., 1991), and are predicted to differ between passive and active muscle stretch. Transition points for individual sarcomeres were identified

computationally using a minimum mean square error algorithm based on linear regression (see Appendix). Only sarcomeres with clear transition points were included in the sarcomere level analysis. When the transition points for proximal and distal segments of the same sarcomere differed by more than 300 nm, data were removed from the analysis. This occurred either when the proximal or distal segments did not reach a transition point (not stretched far enough) or the transition point was not prominent enough for proximal or distal segments to be characterized by the algorithm. This criterion eliminated 25% of active and 64% of passive sarcomere transition point data. No grouped myofibril or pooled myofibril level data were eliminated.

We observed that the initial SL of the myofibrils was correlated with the transition point during active stretch, and also weakly during passive stretch. Thus, movements were grouped into 200 nm windows and analyzed based on the SL window at the beginning of stretch. Data were organized in three ways: (1) individual sarcomere data were grouped by SL at stretch onset; (2) individual myofibril data were grouped by average SL at stretch onset; and (3) all myofibril data were pooled regardless of SL. For each type of analysis, 100 nm bins were averaged to represent the sarcomere data and grouped or pooled myofibril data.

Statistics

One-way ANOVA was used to compare proximal and distal segment lengths during passive and active stretch ($\alpha=0.05$).

RESULTS

Sarcomere data

In addition to measuring segmental extension in passive muscle, here we also report observations of segmental extension in calcium-activated myofibrils. Proximal and distal segment lengths behaved differently during passive and active stretch.

For passive stretching, proximal and distal segments of titin elongated continuously and predictably following the known segmental stiffness properties. For active stretching, proximal titin segment elongation was greater and distal titin elongation was smaller initially (up to an average SL of 3.0 µm) compared with the passive condition, while the reverse was true at SL greater than about 3.0 µm on average (Fig. 1C,D).

We observed that while the amount that sarcomeres shortened varied with calcium activation, there was a linear relationship between the initial SL immediately before stretch (SL bin) and the SL at which the transition point was observed (Fig. 2). Shorter initial SLs resulted in earlier transition points for proximal and distal segments. As the location of the active transition points was largely dependent on the length at which stretch began, we grouped sarcomere transition points by stretch onset for passive and active sarcomeres (Figs 2 and 3). Nearly all proximal and distal segment contour lengths were achieved at shorter SLs during active compared with passive stretch (Fig. 2, left and right). Additionally, active distal segment contour lengths were themselves shorter than passive distal segment contour lengths for almost all sarcomeres at the transition point. For active sarcomeres, 122 of 149 exhibited distal segment lengths of close to 0 nm at the transition point (Fig. 2, right). The location of sarcomere transition points determined using the regression algorithm (Fig. 2) was qualitatively similar to that of the myofibril transition points where no algorithm was applied (Fig. 3B). This suggests the elimination of sarcomeres based on the algorithm criteria (see Materials and methods) had little, if any, effect on the determination of the SL at which the transition point occurred.

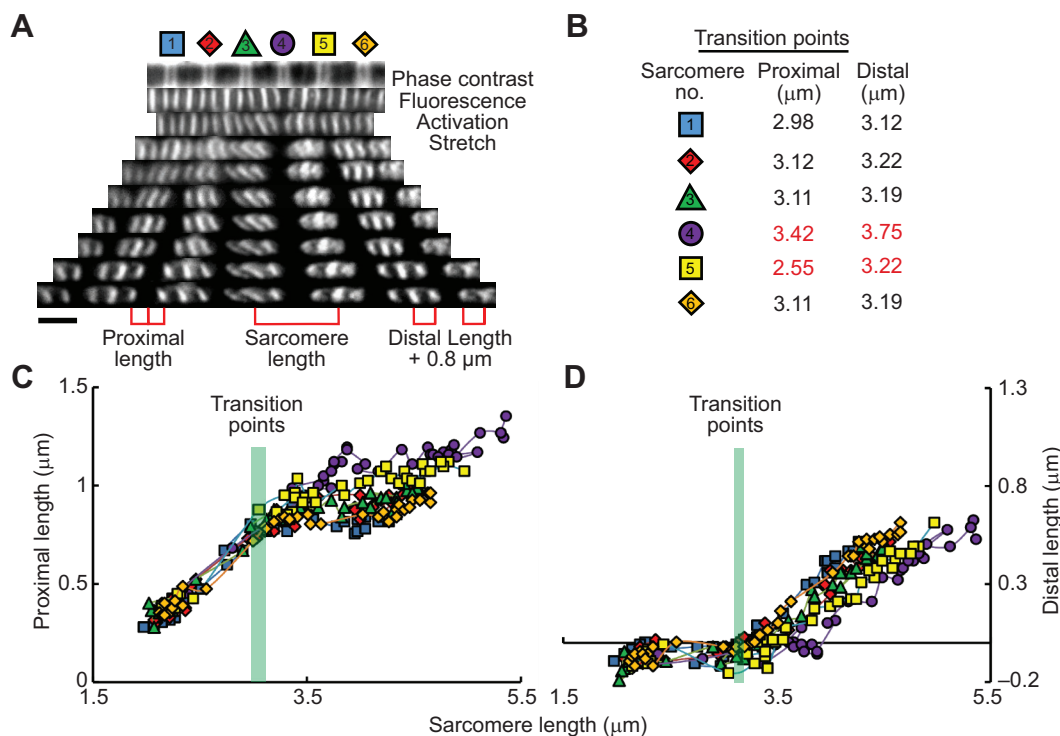


Fig. 1. Elongation of proximal and distal titin segments during active stretch of a six-sarcomere myofibril. (A) Segment and sarcomere lengths (SLs) were derived from measurements as highlighted in red. Scale bar: 2 μm. (B) SLs of transition points for proximal and distal segments, with those eliminated highlighted in red. (C) Proximal segment lengths and (D) distal segment lengths of the six sarcomeres during active stretch with the transition point range highlighted in green. Note that proximal lengths increased largely before the transition point, while distal lengths increased after.

Grouped myofibril data

Proximal and distal segments were observed to elongate linearly with passive stretch until approximately 3.5 μm average SL, while active stretch resulted in elongation patterns dependent on the initial SL of stretch (Fig. 3). Calcium activation prior to stretch resulted in rapid shortening of the distal segment, leaving the proximal segment relatively unchanged (Fig. 3C). As a result, active distal segment lengths were negative for nearly all SL groups prior to the transition points, which was strikingly different from the passive condition.

Pooled myofibril data

The active proximal (Fig. 4, left panel, red) and distal (Fig. 4, right panel, red) lengths were significantly different ($*P=0.002$, $**P<0.001$) from the passive proximal and distal lengths (Fig. 4,

left and right panels, respectively, green). Note that the slope of the active proximal segment length change was larger than that of the passive proximal segment up to an average SL of 2.7 μm. Beyond 2.7 μm, the slope of the active distal segment length was larger than that of the passive distal length, which also coincided with the distal length becoming positive.

Segment length measurements

Segment lengths were obtained from Fig. 4 data for passive and active stretch of proximal and distal titin segments (Fig. 5). During active stretch, the proximal segment was 134 nm longer than during passive stretch at an average SL of 2.7 μm. At a SL of 3.5 μm, this difference diminished to 62 nm between active and passive proximal segment lengths.

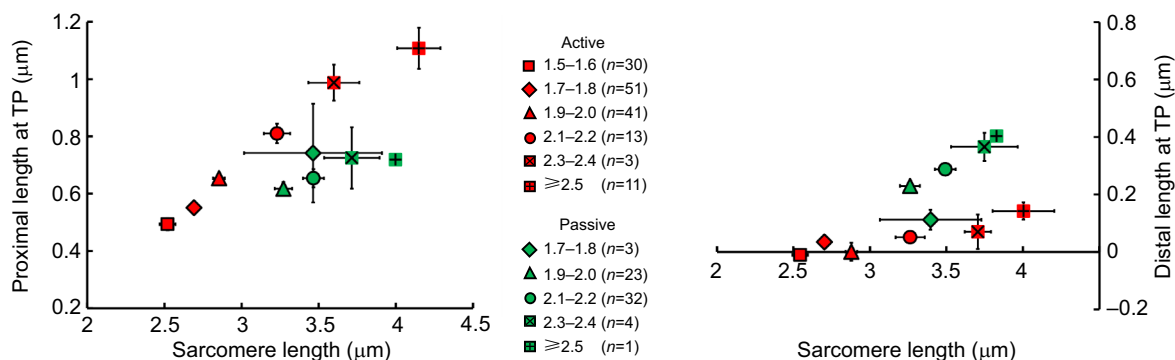


Fig. 2. Length of proximal and distal titin segments during passive and active stretch at the transition point. Sarcomere data were arranged into 200 nm groups based on SL at stretch onset for active (red) and passive (green) sarcomeres for the proximal (left panel) and distal (right panel) segments. TP, transition point. All points are means \pm s.e.m. Note that 55 of 63 passive sarcomeres are represented by the triangle and circle, and 122 of 149 active sarcomeres are represented by the square, diamond and triangle.

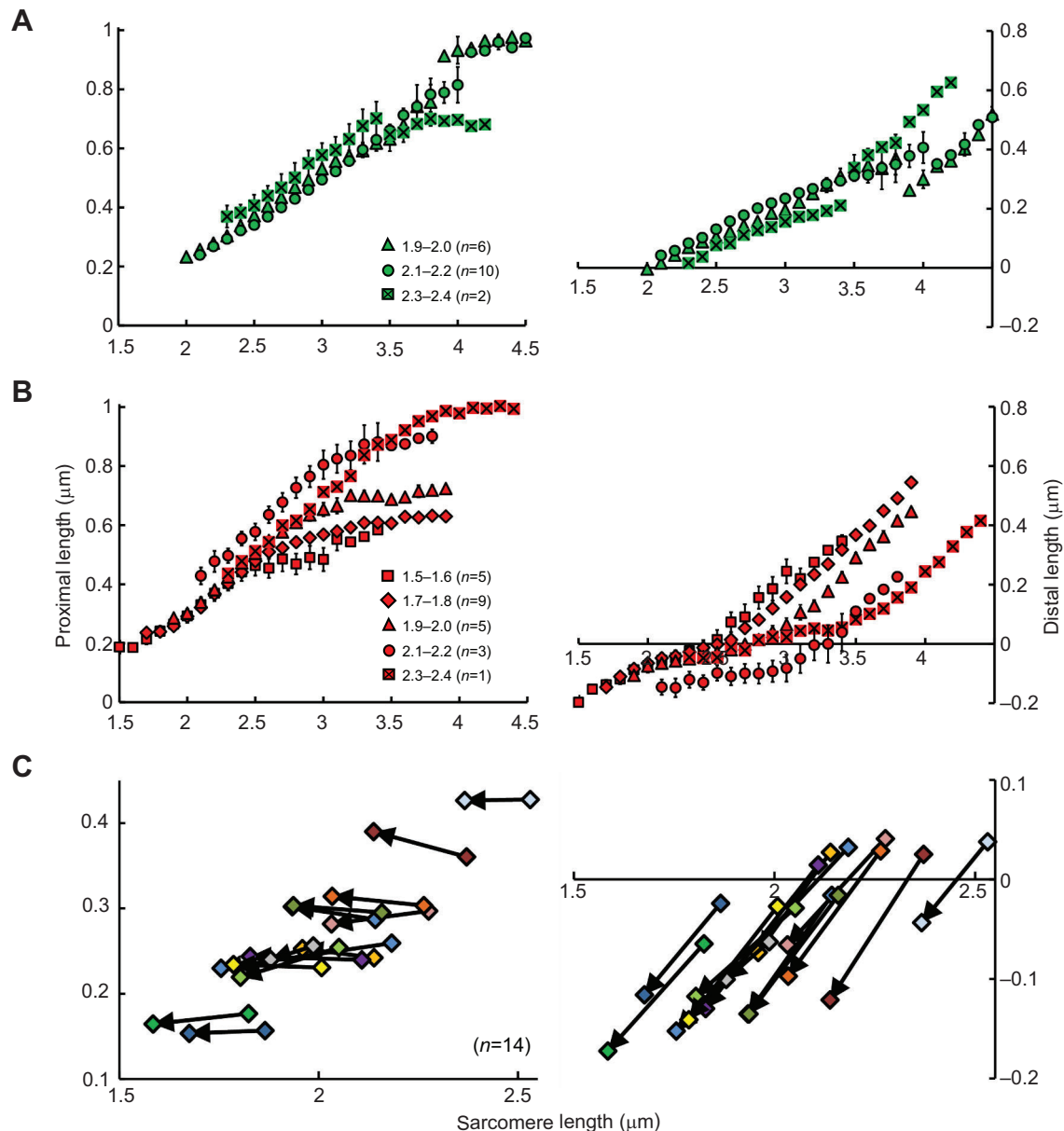


Fig. 3. Myofibril data during passive and active stretch when grouped by stretch onset. (A) Passive ($n=18$, green) and (B) active ($n=23$, red) stretch of the proximal (left) and distal (right) segments of titin based on 200 nm initial SL bins. All points are means \pm s.e.m. (C) Proximal (left) and distal (right) segment length changes immediately before (end of arrow) and after (tip of arrow) activation. Note that proximal lengths were largely unaltered upon activation but distal lengths underwent unanimous shortening into the A-band space (region below a distal length of 0 μ m).

DISCUSSION

This work used segmental elongation of titin during passive and active skeletal muscle stretch to evaluate titin and actin binding as a possible mechanism for residual force enhancement. We measured titin I-band segments before and during passive and active stretch, focusing on regions of titin proximal and distal to the PEVK segment, proposed as a possible site for calcium-dependent actin interaction (Kulke et al., 2001; Nagy et al., 2004; Niederländer et al., 2004).

Passive stretch to approximately 3.5 μ m was typically required to fully stretch individual Ig domains as well as the PEVK region to segment contour lengths (the transition points) for psoas muscle (Figs 2 and 3A), as also found by others (Linke et al., 1998a). Up to this average SL, passive myofibrils (and sarcomeres) showed uninterrupted linear elongation of proximal and distal titin segments

(Figs 3A and 4). At 3.5 μ m, the experimental segment lengths resembled predicted segment length calculations, assuming 5 nm per Ig domain and 0.34 nm per 1400 PEVK amino acid residues (Labeit and Kolmerer, 1995; Linke et al., 1998b). In this case, the theoretical proximal segment length was 667 nm (650 nm obtained experimentally), while the distal segment length was 269 nm (295 nm obtained experimentally) at a SL of 3.5 μ m.

This study is the first to evaluate titin segment behavior upon activation in muscle myofibrils. Several noteworthy observations were made for proximal and distal segment lengths: (1) upon activation, (2) during stretch to the transition point, and (3) during stretch beyond the transition point (see below). Transition points, reflecting attainment of segment contour lengths, were compared in the presence and absence of calcium to determine whether segmental elongation changed upon activation.

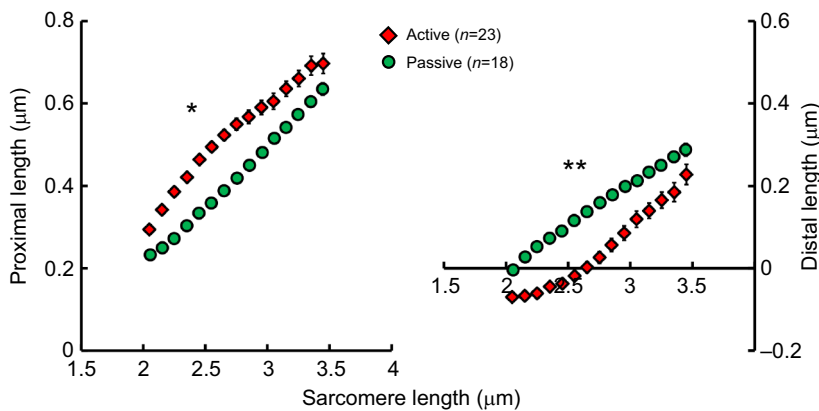


Fig. 4. Pooled data for proximal (left) and distal (right) titin I-band segments from all passive and active myofibrils. All points are means \pm s.e.m. (ANOVA, * $P=0.002$, ** $P<0.001$). Note that the largest difference occurred at a SL of 2.7 μm , and diminished thereafter. Pooled myofibrils are those from Fig. 3, with no sorting by initial SL.

Activation

Prior to stretch, myofibril activation consistently decreased the length of distal segments to values less than zero, with little change in the length of proximal segments (Fig. 3C). Because the zero length of the distal segment indicates the edge of the A-band, shortening of distal segments to negative lengths suggests that titin's distal segment was pushed into the A-band lattice space upon calcium activation. When sarcomeres shortened, proximal segment movement may have been limited by the Z-line (Fig. 3C, left) (Horowitz et al., 1989). Conversely, unoccupied lattice spacing in the A-band region of shortening sarcomeres may have resulted in titin movement into the A-band region, translating into distal lengths of less than 0 μm (Figs 1D, 3B,C and 4). This titin behavior was also observed by others when activated psoas sarcomeres had I-band lengths less than 0.1 μm upon sarcomere shortening (Horowitz et al., 1989).

Stretch to transition point

At the onset of active stretch, the distal segment overlapped spatially with the A-band, and the length of the distal segment changed little prior to the transition point (Figs 1D, 3B and 4). In contrast to the stationary distal segment, the proximal segment elongated considerably, moving the titin antibody away from the Z-line. This increase in proximal segment length appeared too large to be explained by Z-line widening (Tonino et al., 2010), and was beyond the passive proximal segment length (650 nm) at times (Figs 1, 2 and 3). To reconcile this, some Ig domains would need to unfold to accommodate proximal segment lengthening during active stretch, which was at times exclusively responsible for the overall increase in SL prior to the transition point (Fig. 1). At the myofibril level, this

pattern of rapid proximal segment lengthening during active stretch was also seen prior to the transition point (Figs 3B and 4). These results contrast with the predicted lack of proximal segment lengthening during active stretch if titin's proximal segment was anchored to actin.

Stretch at and beyond the transition point

With active stretch, titin's transition points generally occurred at shorter SLs than with passive stretch (Fig. 2), supporting the hypothesis that titin proximal and distal segments extend differently during passive versus active stretch. The difference between active and passive transition points for proximal and distal titin segments was evident in all analyses including sarcomeres, and grouped and pooled myofibrils, indicating that the observed changes in segmental elongation with calcium activation are a consistent feature. Sarcomere and myofibril behavior, grouped by SL at active stretch onset, often displayed a transition point that coincided with a distal length close to zero (Figs 3 and 4B). This suggests that active distal titin lengths only begin to increase substantially when they re-enter the I-band with sufficient stretch, which was completely different from the passive distal lengths irrespective of any SL grouping (Figs 3 and 4A, right). It has been shown that sarcomere labeling before passive stretching, or passive stretching first and then labeling, result in virtually the same label movement (Linke et al., 1996). Thus, it is unlikely the antibody labels themselves change titin's ability to elongate with stretch. Additionally, a pause of 10 min between stretches was sufficient to recover label movement both passively and actively (data not shown), suggesting that no permanent damage occurred to titin from the stretch protocol.

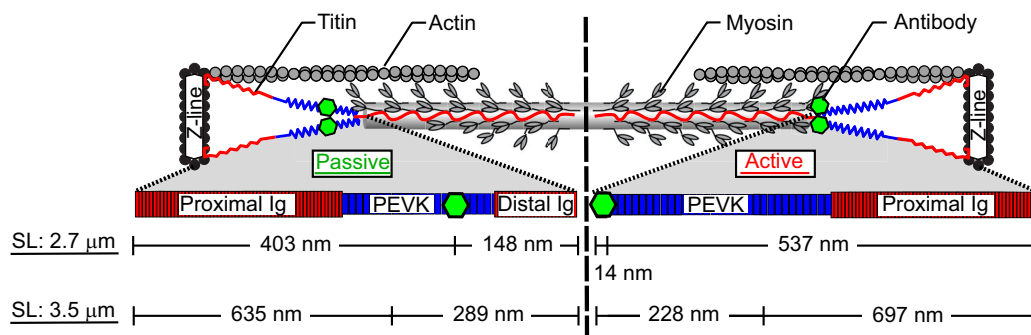


Fig. 5. Proximal and distal segment lengths for active and passive stretch at a SL of 2.7 and 3.5 μm . Note that the active distal segment length is 10% the passive distal segment length at 2.7 μm , resulting in a 134 nm increase in the proximal segment length. At a SL of 3.5 μm , the F146 antibody is shifted 62 nm towards the center of the sarcomere in active compared with passive stretch. Length measurements are not drawn to scale.

Segment lengths were further compared at two average SLs: the overall active transition point (2.7 μm , Fig. 4) and the overall passive transition point (3.5 μm , Fig. 4). At an average SL of 2.7 μm , we calculated the length of the proximal Ig domains from the center of the Z-line to the beginning of the PEVK region as 350 nm (50 proximal Ig at 5 nm each and half the Z-line width plus the actin-bound titin near the Z-line – 100 nm), which is similar to values seen experimentally by others (~360 nm), using the N2A antibody in psoas tissue (Linke et al., 1998a). The length of this Ig domain region is largely unchanged ($\leq 10\%$) during passive stretch from 2.7 μm to 3.5 μm (Linke et al., 1998a). In a similar manner, the theoretical length of the distal segment is 110 nm (22 Ig domains at 5 nm each), and assumed to change little during passive stretch from 2.7 μm to 3.5 μm . With this, the PEVK length can be calculated once Ig domains are fully straightened ($\text{SL} \geq 2.7 \mu\text{m}$), and this length can be compared between passive and active stretch to investigate possible titin PEVK–actin binding. Assuming 1400 residues for psoas PEVK (at 0.34 nm per residue), then the theoretical PEVK contour length would be 476 nm (Linke et al., 1998b).

Using the above assumptions, we obtained an average experimental PEVK length of 91 nm during passive stretch (551 nm total length from Z-line to A-band edge, minus 460 nm for straightened proximal and distal Ig domains) and ~180 nm (537 nm proximal length minus 350 nm proximal Ig domains) during active stretch at 2.7 μm (see Figs 4 and 5). As the distal segment length was 14 nm, distal straightening did not occur, requiring further PEVK extension to accommodate muscle lengthening at 2.7 μm . Given that initial SL affected the proximal segment length at the transition point, the proximal segment PEVK portion (2/3 of total PEVK length) varied between 134 and 327 nm at a SL of 2.7 μm during active stretch (from Fig. 3B), suggesting that the PEVK region can be more than 3.5 times longer in active than in passive stretch of the proximal segment.

With further stretch to 3.5 μm , the PEVK length converged between passive and active myofibril conditions (Fig. 5, 464 nm passively and 465 nm actively), and resembled the theoretical PEVK length when fully straightened (476 nm). Interestingly, however, the proximal and distal segment lengths were not equivalent between passive and active stretch, with the F146 label being located 61 nm closer to the M-line during active stretch. As this would exceed theoretical PEVK lengths, it seems more likely that proximal Ig domains unfolded to accommodate the antibody movement towards the M-line, as proposed earlier. This is further supported by recent work suggesting titin Ig domain unfolding occurs at physiological SLs (Jaime André Rivas-Pardo et al., 2016; Kellermayer et al., 1997).

Titin–actin

This leads us to speculate what may be going on mechanistically when sarcomeres are activated and stretched. As calcium-dependent increases in titin stiffness alone (DuVall et al., 2013; Labeit et al., 2003) do not appear large enough to explain the increased force seen following eccentric contractions (Leonard and Herzog, 2010; Powers et al., 2014), a shortening of titin's distal segment could in theory explain this enhanced force. The mechanical interaction between titin and myosin end filaments may serve to shorten the distal Ig and part of the PEVK region of titin, which would increase titin stiffness and thus titin's force in response to active stretch without requiring additional energy. The observations we report here are consistent with previous studies which argue that titin's length (and stiffness) change upon activation (Leonard and Herzog, 2010; Linke et al., 1997; Nishikawa et al., 2012), but in a manner

that has not been observed before. At the level of the sarcomere, myofibril and pooled data collected here, the proximal length of titin increased considerably with active stretch, while the distal length was often negative prior to the transition point. The coinciding of the distal length transition point with the edge of the A-band would suggest this region has limited mobility prior to the proximal length achieving its segment contour length. Beyond the transition point, the distal length increased significantly more than during passive stretch, ultimately behaving in the opposite way to that expected if titin were bound to actin in the PEVK region. If titin's PEVK region were bound to actin, little change to the proximal length of titin would be expected during active stretch, owing to actin anchoring (Leonard and Herzog, 2010) or possibly winding (Nishikawa et al., 2012). Although titin PEVK interaction with actin has been shown using various methods, it appears to be abolished in the presence of calcium (Kulke et al., 2001) or with calcium/S100A1 (Yamasaki et al., 2001), supporting our observations that the PEVK region did not interact with actin during active stretch.

In the pooled myofibril data (Fig. 4), the largest deviation between passive and active segment extension occurred at the midpoint of the physiological SL range for this muscle (2.7 μm) (Goulding et al., 1997). The short distal segment length, and minimal movement with stretch below the average active transition point (2.7 μm), would suggest that titin was shortened. The first 350 nm per half sarcomere of passive elongation from a SL of 2.0 to 2.7 μm is dedicated to straightening Ig domains, generating little force in the process (Linke et al., 1998a,b). The active shortening of the distal titin segments would appear to eliminate roughly 30% of Ig domain straightening (22 Ig domains of 77 total in rabbit psoas I-band titin; Freiburg et al., 2000), which would require PEVK-dependent force generation to occur at shorter SLs when compared with passive stretch at the same SLs. These data resemble residual force enhancement experiments by Edman et al. (1982), who observed that the augmented residual force was largest at SLs between 2.8 and 3.0 μm in single frog fibers, and diminished thereafter. The weakening enhanced force could reflect the convergence of proximal and distal titin segment lengths at SLs beyond the average active transition point (2.7 μm). However, this conflicts with sarcomere data for sarcomeres pulled well beyond actin and myosin filament overlap (Leonard and Herzog, 2010; Powers et al., 2014). As passive and active proximal and distal titin segments begin to converge at long SLs (extrapolation of Fig. 4), any increased force due to segment shortening would presumably be eliminated. Although these long lengths were not the objective of our experiments, the contradiction is noteworthy and may suggest a mechanistic change in titin behavior when Ig domain unfolding or recruitment of inextensible titin from the A-band (Wang et al., 1991) become prominent (beyond actin–myosin filament overlap).

Interestingly, the initial length of the distal segment in resting passive sarcomeres was also approximately zero, suggesting that the F146 epitope and distal I-band titin are often located at the A-band edge (Fig. 4, right). This proximity, when paired with muscle shortening resulting from activation, moved titin into the A-band space (Fig. 3C) (Horowitz et al., 1989). This could conceivably lead to entanglement of the contracted titin filaments by rotating cross-bridges that project 60 degrees upward from the thick filament axis (Reconditi et al., 2011). This idea could then further explain part of the cross-bridge dependence known to be critical to the underlying mechanism of force enhancement. When active stretch experiments were performed while preventing the cross-bridge working stroke, the enhanced force with stretch was one-quarter of the increase seen when cross-bridges were permitted to contribute to force production

(Joumaa et al., 2008a). At this time, however, there is little support for any biochemical affinity of myosin heads for I-band titin (Li et al., 1995; Murayama et al., 1989; Niederländer et al., 2004), leading us to believe any interaction is mechanical in nature. Myosin-binding protein C (MyBP-C), known to couple titin and myosin, is likely not responsible for the observed overlap between I-band titin and the A-band, as MyBP-C does not overlap spatially with the thick filament ends in the sarcomere called the D-zone (Labeit and Kolmerer, 1995).

The consistent difference between active and passive titin segment elongations requires careful study with published epitopes, which is currently underway. Antibody epitopes targeted to either side of F146 using titin 9D10 and 891 maintained a similar pattern of antibody movement into the A-band space upon activation (DuVall, 2015), suggesting this is not unique to the F146 antibody used in this study, but the unknown binding site of F146 is a study limitation. Additionally, our analysis and interpretation require constant filament lengths, highlighting a further limitation of this study should the thick filament not remain 1.6 μm long throughout contraction and stretch. The observations of titin's distal segment being found in the A-band requires careful further examination, but the consistent difference between passive and active proximal and distal segments across all analyzed levels suggests that titin shortening is occurring in the distal region of titin at physiological SLs and in a SL-dependent manner. The degree to which this interaction was maintained depended on how much shortening occurred prior to active stretch, and was markedly different from passive stretch in all observed cases. In time, we will be able to characterize other I-band segments of titin upon muscle activation and stretch to unearth the role of this molecular spring in active muscle contraction, and expand current two-filament theories of muscle contraction.

APPENDIX

Algorithm parameters

We used a three-line model to describe the distance from one F146 epitope on titin to the other F146 epitope (across the Z-line) as a function of time. For any two given time points where $t_1 \leq t_2$, we calculated three lines by linear regression: (1) from the start of stretch to point t_1 ; (2) from point t_1 to point t_2 ; (3) from point t_2 to the end of stretch.

The following constraints were applied to all sarcomere elongation traces: point t_1 was the intersection of the first two lines, point t_2 was the intersection of the last two lines, and the third line had a slope of zero. The two points with the minimum mean square error combination were used as t_1 and t_2 .

To determine the transition point for distal titin segments, a two-line model based on linear regression was used as a function of SL: (1) from the start of stretch to point s_1 ; (2) from point s_1 to the end of stretch.

The end node of the first line was the same as the start node of the second line. The SL corresponding to the time or SL location of proximal and distal segments was compared, and if they were within 300 nm of one another, the sarcomere transition point was retained. For passive stretches, the transition point was more subtle as the two titin segments elongated simultaneously, which was not usually the case for active stretch prior to a transition point.

Acknowledgements

We thank Dr Nishikawa for her critical review of the experimental data and manuscript preparation.

Competing interests

The authors declare no competing or financial interests.

Author contributions

Conceptualization: M.M.D., T.L., W.H.; Methodology: M.M.D., A.J., T.L.; Software: A.J., G.S.; Formal analysis: M.M.D., A.J., G.S., W.H.; Investigation: M.M.D., W.H.; Resources: W.H.; Writing - original draft: M.M.D.; Writing - review & editing: M.M.D., G.S., W.H.; Visualization: M.M.D., A.J., G.S.; Supervision: T.L., W.H.; Project administration: W.H.; Funding acquisition: W.H.

Funding

This research was funded by Alberta Innovates Health Solutions, Natural Sciences and Engineering Research Council of Canada, the Canada Research Chairs Programme, the Killam Trusts.

References

- Abbott, B. C. and Aubert, X. M. (1952). The force exerted by active striated muscle during and after change of length. *J. Physiol.* **117**, 77–86.
- Colomo, F., Piroddi, N., Poggesi, C., te Kronnie, G. and Tesi, C. (1997). Active and passive forces of isolated myofibrils from cardiac and fast skeletal muscle of the frog. *J. Physiol.* **500**, 535–548.
- DuVall, M. M. (2015). Titin regulation of active and passive force in skeletal muscle. *PhD thesis, University of Calgary.*
- DuVall, M. M., Gifford, J. L., Amrein, M. and Herzog, W. (2013). Altered mechanical properties of titin immunoglobulin domain 27 in the presence of calcium. *Eur. Biophys. J.* **42**, 301–307.
- Edman, K. A., Elzinga, G. and Noble, M. I. (1978). Enhancement of mechanical performance by stretch during tetanic contractions of vertebrate skeletal muscle fibres. *J. Physiol.* **281**, 139–155.
- Edman, K. A., Elzinga, G. and Noble, M. I. (1982). Residual force enhancement after stretch of contracting frog single muscle fibers. *J. Gen. Physiol.* **80**, 769–784.
- Freiburg, A., Trombitas, K., Hell, W., Cazorla, O., Fougereousse, F., Centner, T., Kolmerer, B., Witt, C., Beckmann, J. S., Gregorio, C. C. et al. (2000). Series of exon-skipping events in the elastic spring region of titin as the structural basis for myofibrillar elastic diversity. *Circ. Res.* **86**, 1114–1121.
- Goulding, D., Bullard, B. and Gautel, M. (1997). A survey of in situ sarcomere extension in mouse skeletal muscle. *J. Muscle Res. Cell Motil.* **18**, 465–472.
- Herzog, W. and Leonard, T. R. (2000). The history dependence of force production in mammalian skeletal muscle following stretch-shortening and shortening-stretch cycles. *J. Biomech.* **33**, 531–542.
- Herzog, W. and Leonard, T. R. (2002). Force enhancement following stretching of skeletal muscle: a new mechanism. *J. Exp. Biol.* **205**, 1275–1283.
- Horowitz, R., Maruyama, K. and Podolsky, R. J. (1989). Elastic behavior of connectin filaments during thick filament movement in activated skeletal muscle. *J. Cell Biol.* **109**, 2169–2176.
- Huxley, A. (1957). Muscle structure and theories of contraction. *Prog. Biophys. Chem.* **7**, 255.
- Huxley, H. E. (1969). The mechanism of muscular contraction. *Science*. **164**, 1356.
- Huxley, H. and Hanson, J. (1954). Changes in the cross-striations of muscle during contraction and stretch and their structural interpretation. *Nature* **173**, 973–976.
- Huxley, A. F. and Niedergerke, R. (1954). Structural changes in muscle during contraction: interference microscopy of living muscle fibres. *Nature* **173**, 971–973.
- Huxley, A. F. and Simmons, R. M. (1971). Proposed mechanism of force generation in striated muscle. *Nature* **233**, 533.
- Jaime André Rivas-Pardo, A., Eckels, E. C., Popa, I., Kosuri, P., Linke, W. A., Fernández, J. M. and André Rivas-Pardo, J. (2016). Work done by titin protein folding assists muscle contraction. *Cell Rep.* **14**, 1339–1347.
- Joumaa, V., Rassier, D., Leonard, T. R. and Herzog, W. (2007). Passive force enhancement in single myofibrils. *Pflügers Arch. Eur. J. Physiol.* **455**, 367–371.
- Joumaa, V., Rassier, D. E., Leonard, T. R. and Herzog, W. (2008a). The origin of passive force enhancement in skeletal muscle. *AJP - Cell Physiol.* **294**, 74–78.
- Joumaa, V., Leonard, T. R. and Herzog, W. (2008b). Residual force enhancement in myofibrils and sarcomeres. *Proc. R. Soc. B Biol. Sci.* **275**, 1411–1419.
- Kellermayer, M. S. Z. and Granzier, H. L. (1996). Calcium-dependent inhibition of in vitro thin-filament motility by native titin. *FEBS Lett.* **380**, 281–286.
- Kellermayer, M. S. Z., Smith, S. B., Granzier, H. L. and Bustamante, C. (1997). Folding-unfolding transitions in single titin molecules characterized with laser tweezers. *Science* **276**, 1112–1116.
- Kulke, M., Fujita-Becker, S., Rostkova, E., Neagoe, C., Labeit, D., Manstein, D. J., Gautel, M. and Linke, W. A. (2001). Interaction between PEVK-titin and actin filaments: origin of a viscous force component in cardiac myofibrils. *Circ. Res.* **89**, 874–881.
- Labeit, S. and Kolmerer, B. (1995). Titins: giant proteins in charge of muscle ultrastructure and elasticity. *Science* **270**, 293–296.
- Labeit, D., Watanabe, K., Witt, C., Fujita, H., Wu, Y., Lahmers, S., Funck, T., Labeit, S. and Granzier, H. (2003). Calcium-dependent molecular spring elements in the giant protein titin. *Proc. Natl. Acad. Sci. USA* **100**, 13716–13721.
- Leonard, T. R. and Herzog, W. (2010). Regulation of muscle force in the absence of actin-myosin-based cross-bridge interaction. *AJP - Cell Physiol.* **299**, C14–C20.
- Leonard, T. R., DuVall, M. and Herzog, W. (2010). Force enhancement following stretch in a single sarcomere. *Am. J. Physiol. Cell Physiol.* **299**, C1398–C1401.

- Li, Q., Jin, J. P. and Granzier, H. L. (1995). The effect of genetically expressed cardiac titin fragments on in vitro actin motility. *Biophys. J.* **69**, 1508–1518.
- Linke, W. A., Ivemeyer, M., Olivieri, N., Kolmerer, B., Rüegg, J. C. and Labeit, S. (1996). Towards a molecular understanding of the elasticity of titin. *J. Mol. Biol.* **261**, 62–71.
- Linke, W. A., Ivemeyer, M., Labeit, S., Hinssen, H., Rüegg, J. C. and Gautel, M. (1997). Actin–titin interaction in cardiac myofibrils: probing a physiological role. *Biophys. J.* **73**, 905–919.
- Linke, W. A., Stockmeier, M. R., Ivemeyer, M., Hosser, H. and Mundel, P. (1998a). Characterizing titin's I-band Ig domain region as an entropic spring. *J. Cell Sci.* **111**, 1567–1574.
- Linke, W. A., Ivemeyer, M., Mundel, P., Stockmeier, M. R. and Kolmerer, B. (1998b). Nature of PEVK-titin elasticity in skeletal muscle. *Proc. Natl. Acad. Sci. USA* **95**, 8052–8057.
- Maruyama, K. (1976). Connectin, an elastic protein from myofibrils. *J. Biochem.* **80**, 405–407.
- Maruyama, K., Murakami, F. and Ohashi, K. (1977). Connectin, an elastic protein of muscle: comparative biochemistry. *J. Biochem.* **82**, 339–345.
- Maruyama, K., Kimura, S., Ohashi, K. and Kuwano, Y. (1981). Connectin, an elastic protein of muscle. Identification of “titin” with connectin. *J. Biochem.* **89**, 701–709.
- Murayama, T., Nakauchi, Y., Kimura, S. and Maruyama, K. (1989). Binding of connectin to myosin filaments. *J. Biochem.* **105**, 323–326.
- Nagy, A., Cacciafesta, P., Grama, L., Kengyel, A., Málnási-Csizmadia, A. and Kellermayer, M. S. Z. (2004). Differential actin binding along the PEVK domain of skeletal muscle titin. *J. Cell Sci.* **117**, 5781–5789.
- Niederländer, N., Raynaud, F., Astier, C. and Chaussepied, P. (2004). Regulation of the actin–myosin interaction by titin. *Eur. J. Biochem.* **271**, 4572–4581.
- Nishikawa, K. C., Monroy, J. A., Uyeno, T. E., Yeo, S. H., Pai, D. K. and Lindstedt, S. L. (2012). Is titin a “winding filament”? A new twist on muscle contraction. *Proc. Biol. Sci.* **279**, 981–990.
- Powers, K., Schappacher-Tilp, G., Jinha, A., Leonard, T., Nishikawa, K. and Herzog, W. (2014). Titin force is enhanced in actively stretched skeletal muscle. *J. Exp. Biol.* **217**, 3629–3636.
- Rassier, D. E. and Pavlov, I. (2011). Force produced by isolated sarcomeres and half-sarcomeres after an imposed stretch. *AJP Cell Physiol.* **302**, C240–C248.
- Reconditi, M., Brunello, E., Linari, M., Bianco, P., Narayanan, T., Panine, P., Piazzesi, G., Lombardi, V. and Irving, M. (2011). Motion of myosin head domains during activation and force development in skeletal muscle. *Proc. Natl. Acad. Sci. USA* **108**, 7236–7240.
- Sugi, H. and Tsuchiya, T. (1988). Stiffness changes during enhancement and deficit of isometric force by slow length changes in frog skeletal muscle fibres. *J. Physiol.* **407**, 215–229.
- Tonino, P., Pappas, C. T., Hudson, B. D., Labeit, S., Gregorio, C. C., Granzier, H., Almenar-Queralt, A., Gregorio, C. C., Fowler, V. M., Bang, M. L. et al. (2010). Reduced myofibrillar connectivity and increased Z-disk width in nebulin-deficient skeletal muscle. *J. Cell Sci.* **123**, 384–391.
- Trombitás, K., Greaser, M., Labeit, S., Jin, J.-P., Kellermayer, M., Helmes, M. and Granzier, H. (1998). Titin extensibility in situ: entropic elasticity of permanently folded and permanently unfolded molecular segments. *J. Cell Biol.* **140**, 853–859.
- Walcott, S. and Herzog, W. (2008). Modeling residual force enhancement with generic cross-bridge models. *Math. Biosci.* **216**, 172–186.
- Wang, K., McClure, J. and Tu, A. (1979). Titin: major myofibrillar components of striated muscle. *Proc. Natl. Acad. Sci. USA* **76**, 3698–3702.
- Wang, K., McCarter, R., Wright, J., Beverly, J. and Ramirez-Mitchell, R. (1991). Regulation of skeletal muscle stiffness and elasticity by titin isoforms: a test of the segmental extension model of resting tension. *Proc. Natl. Acad. Sci. USA* **88**, 7101–7105.
- Yamasaki, R., Berri, M., Wu, Y., Trombitás, K., McNabb, M., Kellermayer, M. S. Z., Witt, C., Labeit, D., Labeit, S., Greaser, M. et al. (2001). Titin–actin interaction in mouse myocardium: passive tension modulation and its regulation by calcium/S100A1. *Biophys. J.* **81**, 2297–2313.